ELECTRIC DIFFERENTIAL WITH SVPWM DIRECT TORQUE CONTROL USING FIVE-LEG INVERTER FOR ELECTRIC VEHICLES

[1]ZULKIFILIE IBRAHIM, [2]NURAZLIN MOHD YAAKOP, [3]MARIZAN SULAIMAN, [4]JURIFA MAT LAZI, [5]AHMAD SHUKRI ABU HASIM, [6]FIZATUL AINI PATAKOR.

[1,3-6]Faculty of Electrical Engineering, Universiti Teknikal Malaysia Melaka, 76100 Durian Tunggal, Melaka, Malaysia
[2]University Kuala Lumpur, Malaysian Spanish Institute, Kulim, 09000, Kulim Hi-Tech, Kedah, Malaysia

ABSTRACT

The stability control of two separate electric vehicle (EV) motors by using only single five-leg inverter (FLI) is the motivation of this study. This paper proposes an electric differential (ED) in a FLI to serve dual separate induction motor (IM) drive-based wheels of an EV traction drive system. FLI is developed to replace the two normal three-phase voltage source inverters that need to independently control the two separate IMs at each of the EV wheels. Stability problem will be tackled by electric differential (ED) algorithm. The proposed traction drive employs space vector pulse width modulation direct torque control (SVPWM DTC) modulator with duty cycle merging algorithm as the switching sequence of the FLI. This technique allowed any portion of DC bus voltage to be allocated to any motor. Simulations were performed. The resulting control performance; speed, torque, and current verified the stability and robustness of the system. This study implies that there is possibility of using only one inverter (FLI) in order to drive two separate IM drive-based wheels without jeopardizes the system stability and robustness.

Keywords: *Electric Vehicle (EV), Five-Leg Inverter (FLI), Electric Differential (ED), Dual Motor.*

1. INTRODUCTION

Recently, two wheels motors traction drives have received an increasing interest in electric vehicle (EV) control systems due to the challenge of having the best stability performance by discovering the ability of the inverters to control the dual separate traction motors [1-4]. Current distribution control of dual directly driven wheel motors has been studied by [1], while [2-3] proposed an adaptive electric differential to the dual wheels drive for electric vehicle motion stabilization. K. Hartani et. *all*, [4] used the behavior model control as the vehicle stability enhancement control for electric vehicle with dual motors drive and A. Nasri et. *all*, [5] used sliding mode control. Many efforts were devoted to the study of multi-motor multi-converters systems (MMS) which many have used two normal three-phase inverters to independently control these two motors as shown in figure 1. The stability and robustness of the system is well performed with

this. However, the MMS presents several drawbacks, such as the increases in space, cost, weight and issues of efficiency of the inverters. A. Emadi et. *all* [6], discussed and emphasized on the importance of reducing the cost of manufacturing of an EV so that it can be well commercialise. This can be achieved by eliminating or reducing the sensors and/or the inverter. Under this argument, this paper proposed new configuration of five-leg inverter to serve the dual wheels motors of traction drive for electric vehicle. The MMS have been replaced with multi-motors single drive systems as illustrated by the block diagram in figure 2. The two motors are independently control from each other by only one single voltage source inverter. Furthermore, in industrial automation research area, multi-motors single drive systems have been introduced long before as one of the solution for these MMS drawbacks. There are few techniques that have been proposed and some have been experimentally realized as example wind and

unwind dual motors centre-driven using five-leg inverter [7].

The chronological of reducing the MMS was started with the multi-motors sharing the DC bus, but each of it has its own VSI, the advantage of not having extra rectifier than to reduce the cost. Later, some of the researchers introduce new circuit topology of having less switches 4 leg and 9 switches [8]. Hence, the cost and complexity can also be reduces. In 2000, Gataric et. *all*, [9] investigated a method shown that, by connecting five-phase stator windings in series in an appropriate manner, it becomes possible to control independently dual motors with the supply coming from a single five-phase VSI. That latter enabled of having only one inverter to control the dual motors independently. As for traction motor for electric vehicle application, there are also attempts done to reduce the number of inverters to control multi-motors by reducing the components; i.e. reduce the switch count [10] from 6 to 4, but the motor use only two-phase power supply, the third leg is connected to both motor by capacitors. While in [11] only introduce the idea of having FLI to control the dual motors in EV and just that, no findings had been reported to date. In this paper, ED will be introduced in FLI traction drive system to independently control the stability of EV.
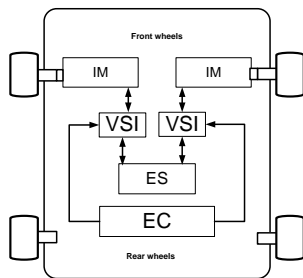

Figure 1. Dual Inverters To Supply Dual Motors EV Traction Drive Configuration (IM: Induction Motor, VSI: Voltage Source Inverter (Normal Three-Phase) As Power Converter, ES: Energy Storage, ECU: Electronic Controller Unit).
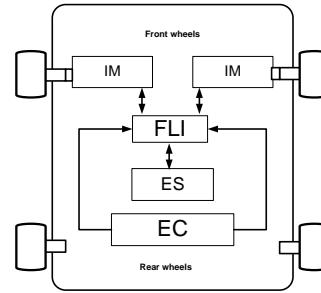

Figure 2. Proposed EV Traction Drive With Five-Leg Inverter Fed Two Separate Induction Motors Configuration (IM: Induction Motor, FLI: Five-Leg Inverter As Power Converter, ES: Energy Storage, ECU: Electronic Controller Unit).

The travel performance of pure EV depends on the performance of its driving system. In this paper, five-leg inverter had been used to replace the normal two three-phase inverter. Other than the cost, this option will also reduce the driveline components, weight and size, thus improving the cost, reliability, and efficiency. Driveline with dual motors requires independent control and an electric differential (ED) to avoid skid and ensure stability [6] both during straight and cornering regime. By using ED, the usage of gear and mechanical differential could be avoided [2]. The ED system plus with FLI will improve the reliability and efficiency of the overall proposed traction system. In this paper, IM has been used as the EV traction-drive [2,6]. Due to its well-known characteristic, direct torque control (DTC) methods appear to be suitable for controlling EV applications [2, 5, 16, 20]. DTC does not need speed and position feedback. The torque, flux and speed are estimated with the value of voltage and current measurements. As to increase the performance of this DTC, SVPWM technique has been applied as the switching sequence control of this DTC. SVPWM DTC had fix switching frequency and also higher voltage utility factor compared to the other classical DTC and PWM techniques [12]. As for FLI the merging duty cycle of SVPWM technique is an improved technique introduce by [8]. SVPWM DTC with merging duty cycle technique specifically for FLI had been proposed by [13 and 14].This will be explained further in section 3.3. Simulation analysis was done. It includes the performance of the speed, torque and current of both motor controls regarding the stability issue. The results can significantly be compared with works done by [2] and [5] that use two inverters to control the two wheel motors.

2.   ELECTRIC VEHICLE DUAL-MOTOR SINGLE INVERTER CONFIGURATION

There are several possible EV drive line configurations [17]. Motor-drive integrated driving mode was the choice for the proposed FLI. The reason is that the motor of this kind driving mode can perform integrated driving axis transmission system with dual motors. It removed the gears and totally realized by electronics controlled. The advantages of this driving mode are; it has compact transmission, high transmission efficiency and easy installation. The ED is connected to the front wheels as depicted in figure 2.

3.   CONTROL OF THE FIVE-LEG INVERTER ELECTRIC VEHICLE DUAL-MOTOR TRACTION DRIVE

The proposed FLI EV dual-motor traction drive control system is as shown in figure 3. In this system, the EV front wheels are associated with ED. The left and right wheels are directly connected to each of the induction motors. The dual-motor are fed by only one inverter, which is the five-leg inverter and controlled by a SVPWM DTC strategy.
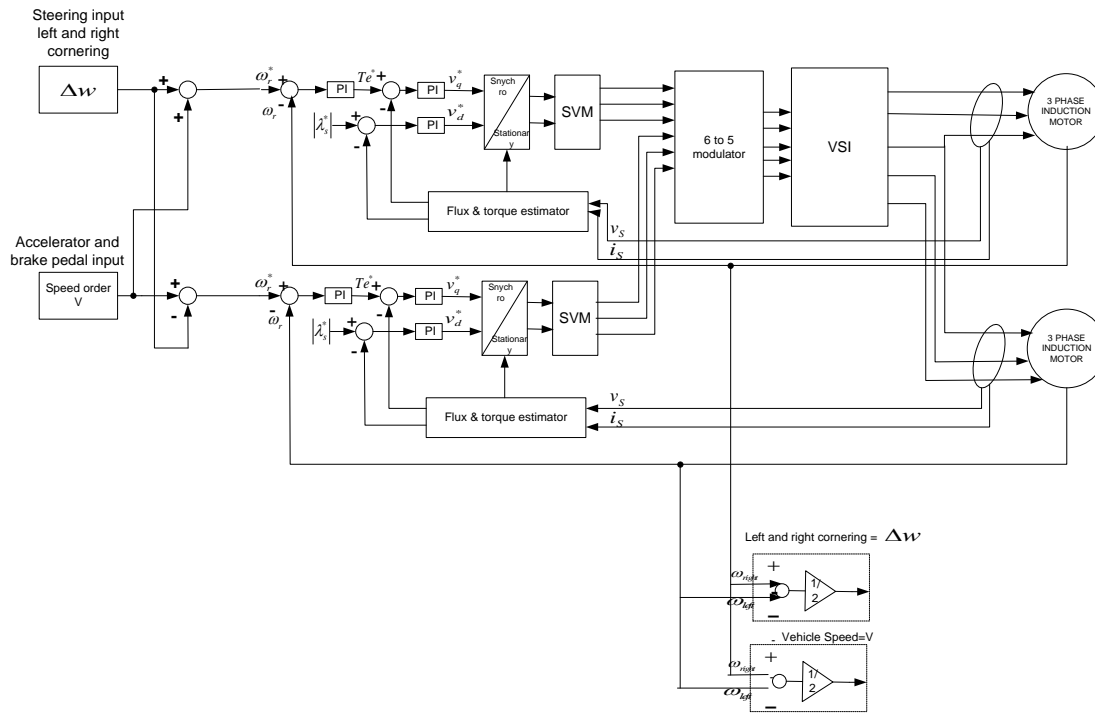

Figure 3. Proposed EV five-leg inverter fed two separate induction motor control system schematic diagram.

3.1.   Stability Control

Speed or torque is the main performance criteria that will show the stability condition of an EV, during straight path and while cornering. The two different wheels will have different speed reference during cornering regime and should maintain the synchronous speed during straight path regime. The easiest method to design ED is the one proposed by Guillermo A. Magallan [19]. It is known as "equal torque strategy" which the principle of this method is to imitate the behavior of a mechanical differential. Thus, this method will always apply same torque to both driven wheels for all vehicle maneuvers. Strategies utilize Ackerman condition were reported to have better ED design. Ackerman condition is a kinematic relation between the outer and inner wheels, this allowing the two wheels turn with slip free [22]. The proposed system as in figure 3 assumes that the vehicle

linear speed or total velocity (*v*) is maintained constant during each maneuver. Therefore, by selecting the desired speed of the vehicle, the DTC torque commands are produced. Each IM rotation speed depends on the selected driving regime type; straight-line regime, the turning regime, and wheel slip-page, where one of the motor experiences almost zero load torque [2 and 14,]. For the straight-path regime, the motor rotation speeds are

$$\omega_l = \omega_r = \frac{v}{r} \qquad (1)$$

For the second regime, cornering regime as shown in figure 4 below, the rotation speeds for each motor are different. For example, in the right turning way, these speeds are expressed as

$$\begin{cases} \omega_l = \dfrac{2v}{\left(1 + \dfrac{\rho + 2d}{\rho - 2d}\right)r} = \dfrac{v}{r} + \Delta\omega \\[4mm] \omega_r = \dfrac{2v}{\left(1 + \dfrac{\rho + d}{\rho - d}\right)r} = \dfrac{v}{r} - \Delta\omega \\[4mm] \Delta\omega = d\dfrac{v}{\rho r} \end{cases} \qquad (2)$$

where $\Delta\omega$ is the speed different between inner wheel and outer wheel. As example right turning, the right wheel is the inner wheel while the left wheel is the outer wheel.
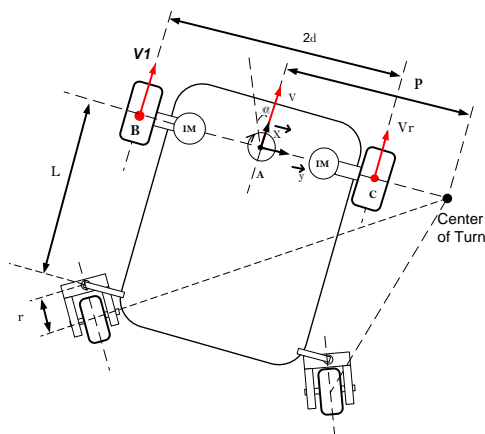
Figure 4.   Electric vehicle driving trajectory model

3.2. Five-Leg Inverter Circuit Topology

Five-leg two-motor drive structure offers a saving of two switches when compared with the standard dual three phase voltage source inverter (VSI) [24 -27]. Thus, it offers a reduction in the inverter structure complexity and also it enable control of two three-phase motors with only one DSP. This advantage can be utilized in the dual traction motors of an EV and there is possibility of reducing the drivelines structure complexity and devices.   Figure 5 shows the main structure of the FLI. The idea of having possible FLI independent control of two motors was first introduced by [23]. The FLI serves two three-phase IMs. Both motors need three inputs, as the results the C leg works as a common leg. Leg A1 and B1 are connected to phase U and V of motor one (M1), while leg A2 and B2 are connected to phase U and phase V of motor 2 (M2) respectively. Switching functions Si (i=1, 2, 3, 4, 5) are defined as Si = 1 when the upper switch is on and Si = 0 when it is off. There are a total of 32 switching states (2^5) in a five-leg VSI, available for control of the two motors [8].
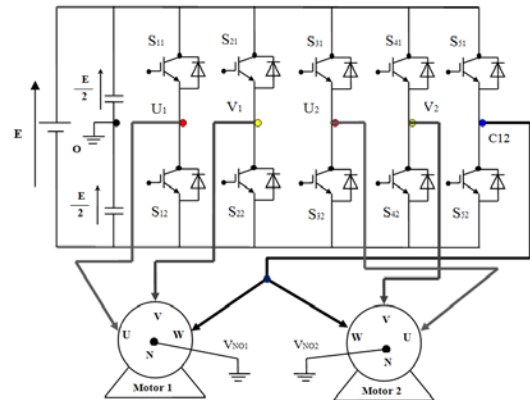
Figure 5. Main Circuit Topology Of Two Three-Phase IM Fed By Five-Leg Inverter.

The maximum voltage value at terminal of an open switch is always equal to the DC voltage V_{DC} (i.e. at rated value such that full operating range of one motor can be achieved). This voltage must be greater than the greatest phase-to-phase voltage. Thus, the capability of FLI leads to a reduction of the supply voltages for the IMs. As the results, speed range and load disturbance that the motors can handle also reduce [13, 26]. The maximum voltage utility factor (v.u.f) (is the rate measurement of the maximum output voltage that can be produce by the inverter and a dc link voltage [29 - 30]) now will depend on the switching technique that will be used to control this FLI.

$$VUF\% = \frac{\sqrt{3}}{2}a_{max}100 \qquad (3)$$

3.3. SVPWM-DTC

Field oriented control and DTC are the two most popular advanced control methods to control the performance of an IM. DTC has simple structure and fast torque response advantages [28]. DTC with space vector modulation (SVM) scheme is proposed in order to improve the classical hysteresis DTC. Paper [12] reported that compared with the steady-state performance of lookup table DTC and SVPWM-DTC, the latter produces much lower torque ripple. This is results from the injection of zero-vector instead of backward active vectors to reduce torque. Another advantage of SVPWM-DTC is it operates at a constant switching frequency.

The behaviour of induction motor in DTC drives principal can be described in terms of space vectors by the following equations written in the stator stationary reference frame:

$$v_s = r_s i_s + \frac{d\varphi_s}{dt} \qquad (4)$$

$$0 = r_r i_s - j\omega_r \varphi_r + \frac{d\varphi_r}{dt} \qquad (5)$$

$$\varphi_s = L_s i_s + L_m i_r \qquad (6)$$

$$\varphi_r = L_r i_r + L_m i_s \qquad (7)$$

$$T_e = \frac{3}{2}P|\varphi_s||i_s|\sin\delta \qquad (8)$$

Where P is the number of pole pairs, ω_r is the rotor electric angular speed in rad/s, L_s, L_r and L_m are the motor inductances, r_s is the stator resistance, [ohm] Ω and δ is the angle between the stator flux linkage and the stator current space vectors. Based on (1) the d^s- and q^s- axis stator flux in the stationary reference frame can be written as:

$$\varphi_{s,d}{}^s = \int\left(v_{s,d}{}^s - i_{s,d}{}^s r_s\right)dt \qquad (9)$$

$$\varphi_{s,q}{}^s = \int\left(v_{s,q}{}^s - i_{s,q}{}^s r_s\right)dt \qquad (10)$$

In terms of switching states S_a, S_b, and S_c (which can either be 0 or 1) the voltage vectors in (7) are given by:

$$v_{s,d}{}^s = \frac{1}{3}V_{dc}(2S_a - S_b - S_c) \qquad (11)$$

$$v_{s,q}{}^s = \frac{1}{\sqrt{3}}V_{dc}(S_b - S_c) \qquad (12)$$

The electromagnetic torque given in (6) can be written in the $d^s – q^s$ coordinates as:

$$T_e = \frac{3}{2}P\left(\varphi_{s,d}{}^s i_{s,q}{}^s - \varphi_{s,q}{}^s i_{s,d}{}^s\right) \qquad (13)$$

The two similar types of three phase induction motors are used in the simulation studies and details about the motor parameters are shown in table 1 below.

Table 1: Induction Motors Parameters

Stator resistance, Rs	7.83Ω
Rotor resistance, Rr	7.55Ω
Stator self inductance, Ls	0.4751H
Rotor self inductance, Lr	0.4751H
Mutual inductance, Lm	0.4535H
Number of poles, p	4
Stator flux rated	0.954
Torque rated	13 Nm
Power	1.5 kW
Speed	1460rpm

There are lots of different PWM methods have been proposed as the switching techniques to the FLI [23], [31]-[33]. Unfortunately by using this conventional PWM the DC bus utilization (v.u.f) is restricted to 50% to each of the motor. As a consequence, many attempts to improve the DC bus utilization with the five-leg topology have been reported [8, 29, 30]. An improved PWM for FLI introduced by [8], for both carrier-based PWM and SV-based PWM (SVPWM) provide solution to the independent control of dual motor even at different speed command and at different load disturbance at same time is possible. With this method the DC bus voltage can easily be allocated to any of the two motors depends on the demand. Improved SVPWM FLI control method was successfully verified by experimental result in [8]. In this paper, the improved SVPWM FLI was applied in the DTC scheme to control this dual traction motor drive with ED. The technique utilizes standard three-phase modulators to generate modulation signals for all legs of a FLI. The end result enables any portion of the DC bus voltage to be allocated to any of the two motors. It produces a symmetrical switching pattern, with identical switching frequency in all the inverter legs. The more interesting factor is that all of the

32 available inverter switching states are utilized. For further understanding, figure 6 shows the block diagram of SVPWM-DTC with PI controllers of one IM drive.
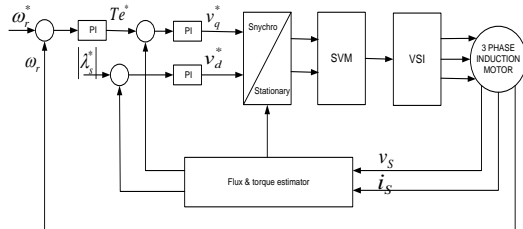

Figure 6. Block diagram of SVPWM-DTC three-phase IM drive.

The basic principle of SVPWM algorithm is it has eight voltage vectors. There are six base vectors has same amplitude and two zero vectors (000) and (111). As shown in figure 7, in the first sector adjacent to the two voltage vector U_1 and U_2 as well as the zero vector can synthesis reference vector U_{ref} in accordance with the method of voltage-second balance.

$$U_1 T_1 + U_2 T_2 + U_0 T_0 = U_{ref} T_S \qquad (14)$$

where T_1 and T_2 are the duration time of active vectors, T_0 is the duration time of zero vectors and T_s is the PWM cycle. From these, the duty cycle of the active vectors and zero vectors are determined.
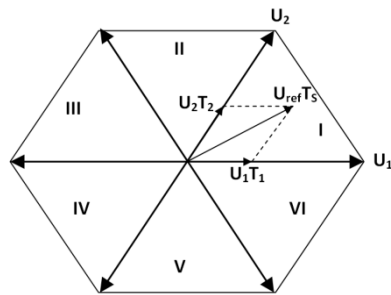

Figure 7. Voltage Vectors And Sectors.

Consider a SV approach to the inverter modeling. Similar principles to those explained in the case of carrier-based PWM [1] of the FLI apply when one considers the SVPWM method for two-motor drive. The existence of zero-sequence signal injection makes it possible for the FLI being able to independently control two three-phase IMs. It is well known that the zero-

sequence signal represents a degree of freedom that is normally used to improve the DC bus utilization and reduce harmonic current losses of the carrier-based method [8]. The zero-sequence signal does not appear in either line-to-line or phase voltages of the three-phase motor. This offer a possibility to utilize the principle of zero-sequence signal injection in a very different manner for a five-leg two-motor drive. Voltage references for each motor are vectors situated in any of the six sectors in their d-q plane of stationary reference frame (as in DTC schemes). Assuming that both modulators are in continuous modulation where total time of application of zero SVs is equally shared among zero SVs 000 and 111, and also the remaining time is determined on average over the switching period of the two adjacent active SV. The three-phase SVPWM modulators will generated the duty cycle values δ over the switching period t_s (time 'ON' over the total switching period) for each of the three legs. A simple summing of the duty cycles generated can be used to determine the resulting five duty cycles for the FLI. That is,

$$\delta_{A_1} = \delta_{a_1} + \delta_{c_2} \qquad \delta_{B_1} = \delta_{b_1} + \delta_{c_2}$$

$$\delta_C = \delta_{c_1} + \delta_{c_2} \qquad (15)$$

$$\delta_{A_2} = \delta_{a_2} + \delta_{c_1} \qquad \delta_{B_2} = \delta_{b_2} + \delta_{c_1}$$

The values of duty cycles calculated by each three-phase SV modulator are in the range (0:1), where the switching period t_s is equal to 1 p.u. Then as in normal SV zero space vector 111 should be injected in the middle of the switching pattern, generated duty cycles will have values equal to 0.5 when the input reference is zero. After summation defined with (5), the FLI duty cycles get shifted into the range (0.5:1.5), which is not applicable with the value of the witching period. Due to this the value from the resulting duty cycles calculated using (15) must continuously subtracted by 0.5. This is shown in figure 8 where the principle of SVPWM for a FLI supplying a two-motor drive is illustrated [8]. The net effect of the duty cycle summation is the redistribution of the application times of the zero SVs. From the first three equations of (15), it is visible that the addition of the value of the duty cycle δ_{c_2} increases all three duty cycles, originally generated by the M1 modulator, in the same manner. Thus, the application time of the zero SV 111 is effectively increased, and as a consequence the application time of the zero SV

000 is decreased (before shifting by – 0.5), without affecting the application times of the two active SVs. The same explanations apply to M2 on the basis of the last three equations of (15). After the application of the SVPWM principle, these sequences and application time durations of active SVs for M1 and M2 stay preserved in the final five duty cycles of the five-leg VSI. It can be further seen that the distribution of the application times for zero vectors 000 and 111 for each of the two machines is different in FLI compared with in M1 and M2, whereas the total zero vector application time (sum of 000 and 111 application times) is kept the same. It is also noticeable that there are instants within the switching period when both machines simultaneously receive their active SVs (overlapped parts, for example, vector 11001 of the five-leg VSI, which corresponds to the active vectors 110 and 010 of the two machines, respectively, since inverter legs A_2 and B_2 supply phases a and b of the second machine while phases c are paralleled to the inverter leg $C_{1,2}$). Thus the individual SV references of each machine are complementary and the modulator is able to simultaneously satisfy the needs of both motors. It is also visible that in the remaining instants the individual SV references of each machine are conflicting and so the needs of one machine are met, whereas the second machine receives zero SV (111 or 000). What this means is that all $2^5=32$ switching states of a five-leg VSI are utilised and there are no restrictions regarding the use of any of them. The resulting PWM pattern is symmetrical with two commutations per inverter leg and is thus easy to implement using standard DSP PWM units.
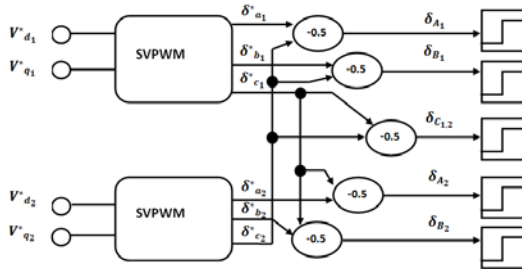

Figure 8. The principal of an improved SVPWM for FLI: the combination of two standard three-phase SVPWM performed five duty cycles signals.

4. SIMULATION RESULTS AND ANALYSIS

The simulations of the proposed ED for FLI with using SVPWM merging duty cycle technique have been done using MATLAB/Simulink. The two IM rated parameter are given in Table 1. Base on the vehicle reference speed profiles [2], two situations of ED performance have been evaluated: 1) the straight path regime, where the two motor have synchronous speed, and 2) the cornering regime, where each motor have different speeds as shown in figure 9 below. The outer wheel moves slower than the inner wheel if the EV needs to perform a cornering regime. As additional we also test the reversed operation of the two wheel motors. These results can literately be compared to works done in [2] and [17], but [17] was using permanent magnet synchronous motors.
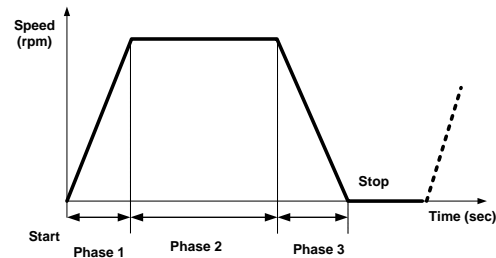

Figure 9. EV speed reference: Phase 1: ramp-up, speed increases linearly, phase 2: constant speed and phase 3: ramp-down, speed decreases linearly.

The first test is the straight path regime. Simulation of the two traction motors having the same speed is shown in figure 10. The speeds are varies synchronously for both motors. In terms of stability the results clearly shown both motors follow accurately the reference speeds trajectory maintaining the synchronous speed. Figure 10(b) show the torque characteristic during straight path regime without load disturbance. From the figure it can be seen that when the speed command is changed from high speed to low speed and vice versa the motors also experienced a slight changes in its electromagnetic torque respond. Figure 10(c) illustrates the phase current of the motors.
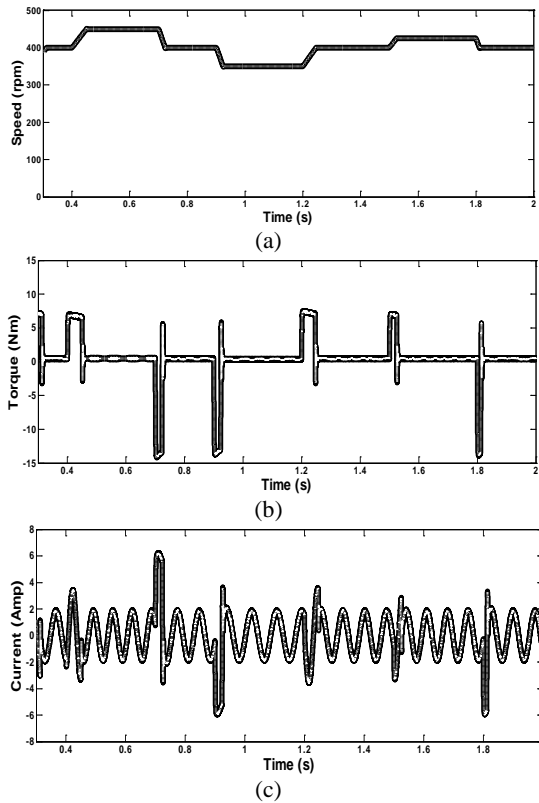
Figure 10. The comparison of simulation results on the first regime: straight path for both motors performance. (a) speed. (b) torque. (c) current.
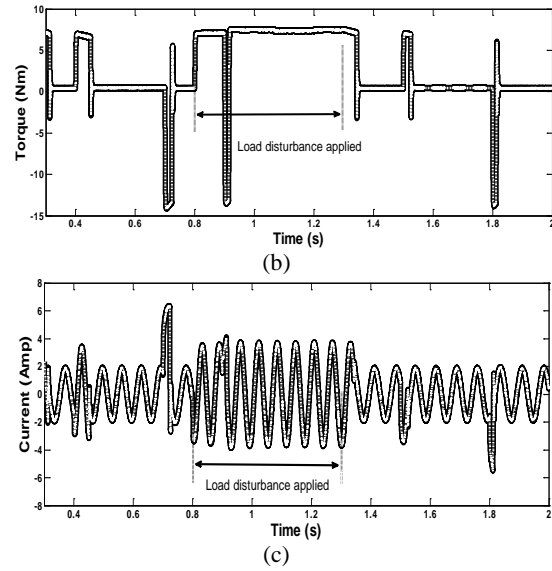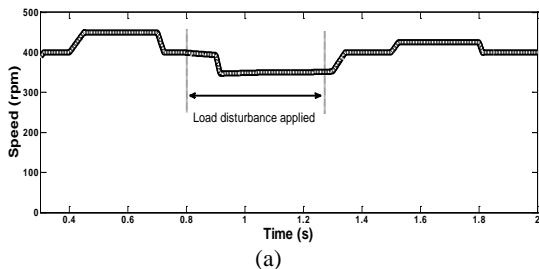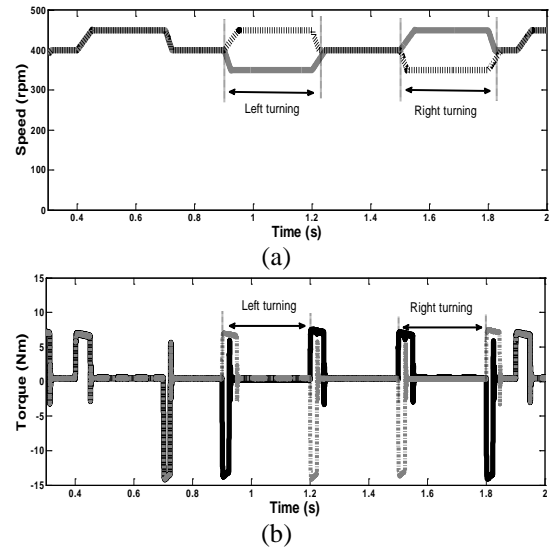

Figure 11. The comparison of simulation results on the load disturbance test of first regime: straight path for both motors performance. (a) speed. (b) torque. (c) current.

The second test is the straight path regime but with some load disturbance. These load disturbances are coming from the external sources such as when the EV passes through a road slope or a bum. Speeds of the driving wheels maintain the same and the road slope do not affect the angular slip control of the wheels. The motor electromagnetic torque is the one having the change, as shown in figure 11. The results of electromagnetic in figure 11(b) can be compared to result of electromagnetic torque in figure 10(b). Since both speeds command are the same but the load disturbance are different so we can clearly see the ability of ED SVPWM DTC controller in stabling the speed of both traction motors.

The third test is the cornering regime test. Both motor initially having the same speed just before taking the cornering. During the cornering, the speed of both motors have slight different where the inner wheel was faster than the outer wheel. ED is the one allowing the different speeds of referent being able to be control significantly.
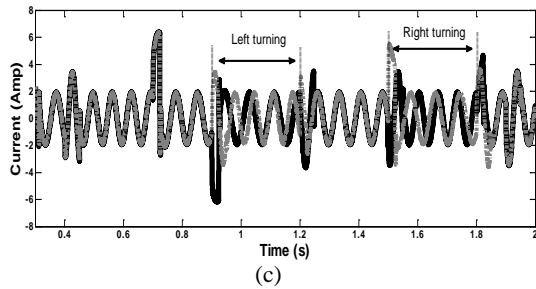
(c)

Figure 12. The comparison of simulation results on the second regime: cornering for both motors performance. (a) speed. (b) torque. (c) current.

The last test done was forward and reversed action plus during the reversed period cornering is applied to the motors. As shown in figure 13 below, the motor ramp up to 400 rpm then at t=0.6s the speed command change to -400 rpm, which make the motors to turn direction. After it reach steady state, the left and right turning regime were applied to both of the motor. The torque and current performance can be seen in figure 13(b) and (c).
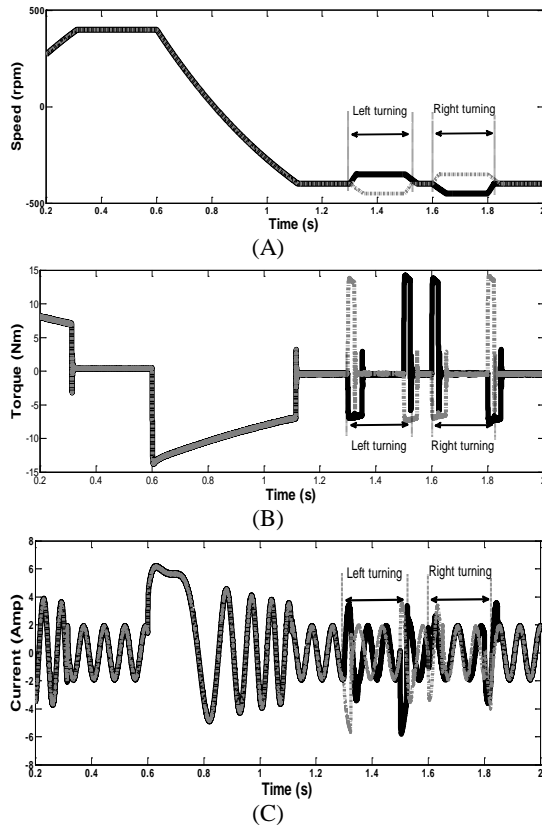

(A)

(B)

(C)

Figure 13. The Comparison Of Simulation Results On The Forward Reversed Operation: Straight Path And Cornering During Reversed For Both Motors Performance. (A) Speed. (B) Torque. (C) Current.

5. CONCLUSION

The focus of this study is the ED performance in FLI SVPWM DTC to control dual motor drive-based wheels of an EV traction drive system. FLI SVPWM DTC with single drive is able to maintain the stability and robustness of an EV. FLI reduced the number of inverter and power supply needed to control two traction motors of an EV. Even though, only with single drive the two motors can be control independently at any speed and at any torque simultaneously. The system is capable of maintaining the stability and robustness of both motors during straight path and cornering regime with or without load disturbance by controlling the delta speed and current also the ability of the merging duty cycle SVPWM technique for FLI to allocate any portion of DC bus to any motors following the demand.

REFERENCES

[1] Y. P. Yang, and C. P. Lo, "Current distribution control of dual directly driven wheel motors for electric vehicles," *Control Engineering Practice*, vol. 16, pp. 1285-1292, 2008.

[2] B. Tabbache, A. Kheloui, and M. E. H. Benbouzid, "An adaptive electrical differential for electric vehicles motion stabilization," *IEEE Trans. Veh. Technol.*,vol. 60, no. 1, pp 104-110, Jan. 2011.

[3] K. Hartani, M. Bourahla, Y. Miloud, and M. Sekour, "Electronic differential with direct torque fuzzy control for vehicle propulsion system," *Turk J Elec Eng & Comp Sci*, vol. 17, pp. 21-38, 2009.

[4] K. Hartani, and Y. Miloud, "Vehicle stability enhancement control for electric vehicle using behavior model control," in book "Electric Vehicles - Modelling and Simulations" edited by Seref Soylu, ISBN 978-953-307-477-1: InTech, September 9, 2011, ch. 6, pp. 127-158.

[5] A. Nasri, A. Hazzab, I. K. Bousserhane, S. Hadjeri, and P. Sicard, "Fuzzy-sliding mode speed control for two wheels electric vehicle drive," *Journal of Elect. Eng. And Technol. (Tubitak)*, vol. 4, no. 4, pp 499-509, 2009

[6] A. Emadi, Y. J. Lee, and K. Rajashekara, "Power Electronics and Motor Drives in Electric, Hybrid Electric, and Plug-In

Hybrid Electric Vehicles," *IEEE Trans. Ind. Electron.,* vol. 55, no. 6, Jun. 2008

[7] M. Jones, D. Dujic, E. Levi, M. Bebic, and B. Jeftenic, "A two motor centre-driven winder fed by a five-leg voltage source inverter," *Proc. European Power Electronics and Applications Conf.* EPE, Aalborg, Denmark, 2007, CD-ROM paper 83

[8] M. Jones, S. N. Vukosavic, D. Dujic, E. Levi, and P. Wright, "Five-leg inverter PWM technique for reduced switch count two-motor constant power applications," *Electric Power Applications, IET,* vol. 2, pp. 275-287, 2008.

[9] S. Gataric, "A polyphase Cartesian vector approach to control of polyphase AC machines," 2000, pp. 1648-1654 vol. 3.

[10] E. Ledezma, B. M. Grath, and A. Munoz, "Dual AC-drive system with a reduced switch count,", *IEEE Transactions on Industry Applications*, vol. 37, pp. 1325-1333, 2001.

[11] M. Jain, and S. Williamson, "Modeling and analysis of a 5-leg inverter for an electric vehicle in-wheel motor drive," *IEEE Canadian Conf. Elect. and Comp. Eng.* (CCECE), pp. 1-5, 2010.

[12] S. Lu, and K. Corzine, "Direct torque control of five-phase induction motor using space vector modulation with harmonics elimination and optimal switching sequence," *IEEE Applied Power Elect. Conf. and Exp.*, pp 195-201, 2006.

[13] N. Mohd Yaakop, Z. Ibrahim, M. Sulaiman and M.H.N. Talib, "Speed Performance of SVPWM Direct Torque Control for Five Leg Inverter Served Dual Three-Phase Induction Motor", *IEEE Int. Power Eng. and Opt. Conf. (PEOCO)*, pp 323-328, 2012.

[14] M.H.N. Talib, Z. Ibrahim, N. Abdul Rahim, and N. Mohd Yaakop, "Development of Combined Vector and Direct Torque Control Methods for Independent Two Induction Motor Drives", *IEEE Int. Power Eng. and Opt. Conf. (PEOCO)*, pp 78-83, 2012.

[15] R. Rajamani, Vehicle Dynamics and Control. Mechanical Engineering Series, New York: Springer, 2006, ch. 1, pp. 8.

[16] J. D. Santiago, H. Bernhoff, B. Ekergard, S. Eriksson, S. Ferhatovic, R. Waters, and M. Leijon, "Electrical motor drivelines in commercial all-electrical vehicles: a

review," *IEEE Trans. Veh. Technol*., vol. 61, no. 2, Feb. 2012

[17] G. Li, W. Hong, D. Zhang, and C. Zhong, "Research on control strategy of two independent rear wheels drive electric vehicle," *Physics Procedia,* vol. 24, pp. 87-93, 2012.

[18] E. Ledezma, B. McGrath, A. Muñoz, and T. A. Lipo, "Dual AC-Drive System with a Reduced Switch Count," IEEE Trans. Ind. Appl., vol. 37, no. 5, pp 1325-1333, Sept./Oct. 2001

[19] C. Fu, R. Hoseinnezhad, Simon Watkins, and Reza Jazar, "Direct Torque Control for Electronic Differential in an Electric Racing Car" School of Aerospace, Mechanical and Manufacturing Engineering, RMIT University, Victoria 3083, Australia

[20] M. H. Westbrook, "The Electric and Hybrid Electric Car". The Institution of Electrical Engineers, pp. 44-47, 2001.

[21] K. Hartani, M. Bourahla, Y. Miloud, and M. Sekour, "Electronic differential with direct torque fuzzy control for vehicle propulsion system," Turk J Elec Eng & Comp Sci, vol. 17, pp. 21-38, 2009.

[22] G. A. Magallan, C. H. D. Angelo, and G. O. Garcia, "Maximization of the Traction Forces in a 2WD Electric Vehicle," IEEE Transactions on Vehicular Technology, pp. 1-1, 2011.

[23] Ph. Delarue, A. Bouscayrol, B. Francois, "Control implementation of a five-leg voltage-source-inverter supplying two three-phase induction machines," *Proc. IEEE Int. Elec. Mach. and Drives Conf. IEMDC*, Madison, USA, 2003, pp. 1909–1915.

[24] Y.Kimura, M.Hizume, K.Oka, and K.Matsuse, "Independent Vector Control of Two Induction Motors with Five-Leg Inverter by the Expanded Two Arm PWM Method", *The 2005 International Power Electronics Conference*, pp.613-616, 2005.

[25] K.Oka, Y.Ohama, H.Kubota, I.Miki, and K.Matsuse: "Characteristic of Independent Two AC Motor Drives Fed by a Five-Leg Inverter ", 2009 *IEEE Industry Applications Society Annual Meeting*, CD-ROM.

[26] E. Levi, M. Jones, S.N. Vukosavic, A. Iqbal, and H.A. Toliyat, "Modeling, control, and experimental investigation of a five-phase series-connected two-motor drive with single inverter supply," *IEEE Trans. Ind. Electron.*, 54, (3), pp. 1504–1516, 2007.

[27] J. M. Lazi, Z. Ibrahim, and M. Sulaiman, "Mean and diffrential torque control using hysteresis current controller for dual PMSM drives," *Journal of Theoretical and Applied Information Technology*, Vol. 33, (1), , pp. 76-82 Nov. 2011

[28] A. Jidin, N. R. N. Idris, A. H. M. Yatim, T. Sutikno, and M. E. Elbuluk, "Extending switching frequency for torque ripple reduction utilizing a constant frequency torque controller in DTC of induction motors," *Journal of Power Electronics*, vol. 11, pp. 148-155, 2011.

[29] K. Oka, Y. Nozawa, and K. Matsuse, "An improved method of voltage utility factor for PWM control of a five-leg inverter in two induction motor drives," *IEEJ Transactions on Electrical and Electronic Engineering,* vol. 1, pp. 108-111, 2006.

[30] A. Dixit, N. Mishra, S. K. Sinha, and P. Singh, "A review on different PWM techniques for five leg voltage source inverter," IEEE Int. Conf. On Adv. In Eng., Sc. and Management, ICAESM 2012, pp. 421-428.

[31] M.Hizume, S.Yokomizo, and K.Matsuse, "Independent Vector Control of Parallel-Connected Two Induction Motors by a Five-Leg Inverter", *10th European Conference on Power Electronics and Applications,* CDROM, paper 778, 2003.

[32] M. Jones, D. Dujic, E. Levi, "A Performance Comparison of PWM Techniques for Five-Leg VSls Supplying Two Motor Drives", IECON- 2008, *The 34nd Annual Conference of the IEEE Industrial Electronics Society*, pp.508-513, CD-ROM, 2008.

[33] B. Francois, A. Bouscayrol: 'Design and modeling of a five-phase voltage-source inverter for two induction motors'. *Proc. Eur. Conf. Power Elec. and Appl. EPE,* Lausanne, Switzerland, 1999, CD-ROM paper 626.